# Whistler-Mode Electron Cyclotron Emission in a Mirror Plasma

R. F. Ellis, G. D. Tsakiris, and D. A. Boyd

*Department of Physics and Astronomy, University of Maryland, College Park, Maryland 20742*

Measurements of electron cyclotron emission in the whistler mode have been made on the Maryland mirror machine and the results are compared with hot-plasma theory. Good agreement is obtained, demonstrating, in particular, that the emission attains black-body levels for a wide range of conditions. It is concluded that this emission is a promising candidate to measure axial variations of the electron temperature in tandem mirror devices.

Electromagentic radiation from plasmas is a valuable tool for understanding plasma behavior and diagnosing plasma conditions.[1] In tokamak plasmas, where the magnetic field $B$ is a function of radius, emission perpendicular to $B$ at the electron cyclotron frequency $\omega_{ce} = eB/m_e$ is used to measure electron temperature $T_e$ as a function of radius.[2] However, a tandem mirror fusion device with thermal barriers[3] requires a $T_e$ which varies axially, i.e., along $B$. No practical diagnostic now exists to measure this variation and its time dependence. An axial array of detectors to measure perpendicular cyclotron emission is too costly and complicated and, for mirror conditions, emission does not attain black-body levels. Likewise, an axial array of laser Thomson scattering setups is costly and complicated and yields an electron temperature at only one point in time. In this Letter we present the first experimental and theoretical results which show that electron cyclotron emission parallel to $B$ in the whistler mode is very promising for this measurement. The whistler mode[4] is well suited because (a) in an axially varying $B$ the condition $\omega = \omega_{ce}$ means that different frequencies correspond to different axial locations; (b) it propagates at high densities ($\omega_p^2 > \omega_{ce}$), where $\omega_p^2 = \epsilon_o n_e e^2/m_e$ and $n_e$ is the plasma

density; (c) emission reaches black-body levels for a wide range of plasma parameters and depends only on the electron temperature and not other parameters such as plasma density. Our results also represent the first confirmation of hot-plasma theory with respect to this fundamental mode of plasma emission and are thus also of general interest.

A schematic of the experiment is shown in Fig. 1. An argon plasma ($n_e = 3 \times 10^9 - 3 \times 10^{12}$ cm$^{-3}$, $T_e = 1-3$ eV) is generated by a pulsed, low-pressure ($p \lesssim 1$ mTorr), hot-cathode discharge (voltage 50–200 V) in a magnetic geometry consisting of a 2-m-long uniform quasistatic bias field of 700 G and a 40-cm-long pulsed mirror field of mirror ratio 1.7 and maximum midplane field of 7 kG.[5] The plasma column fills the length of the machine and has a radius of approximately 2 cm at midplane. Plasma density is measured with Langmuir probes and an 8-mm microwave interferometer; electron temperature is measured with Langmuir probes. Nonthermal electrons are measured using a gridded energy analyzer. Radiation traveling along the axis is received by a high-gain horn and detected by a 12–18-GHz superheterodyne receiver (minimum detectable signal ~ 0.1 pW, IF bandwidth 25 MHz). During a
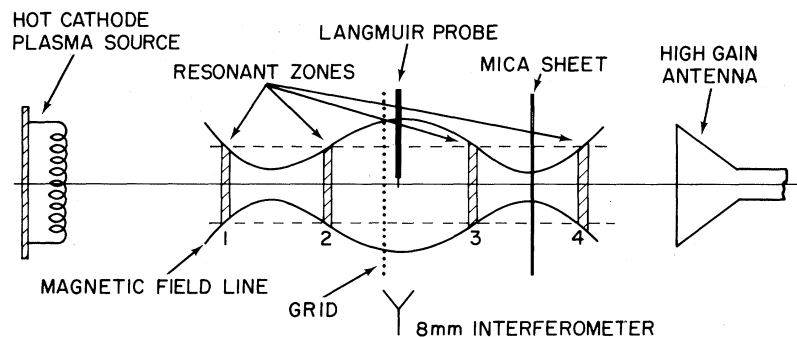


FIG. 1. Schematic of experimental setup. Drawing not to scale: mirror-mirror distance, 40 cm; midplane-horn distance, 71 cm; midplane-source distance, 74 cm. Mica sheet and grid may be moved to different axial locations.
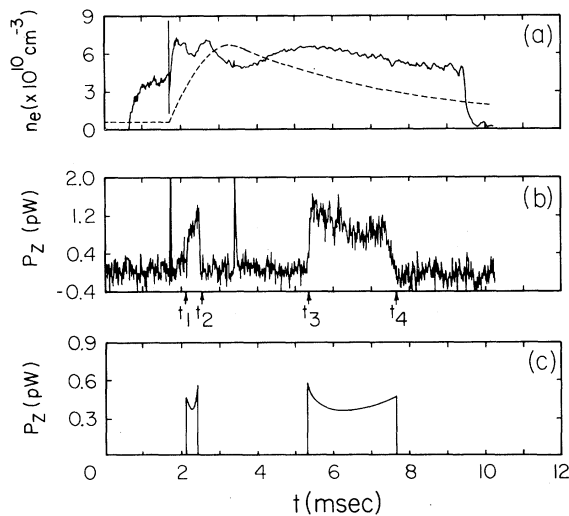
FIG. 2. Typical data shot at discharge voltage of 100 V, pressure 0.3 mTorr, and $T_e$ = 3 eV. (a) Plasma density (solid line), magnetic field (dashed line) with peak $B$ = 7.74 kG. (b) Measured microwave emission; $t_1$, $t_2$, $t_3$, $t_4$ explained in text. The large spikes at 1.8 and 3.4 ms are noise from ignition firing; the "hash" is thermal noise in the detection system. (c) Prediction of theoretical model based on hot-plasma theory.
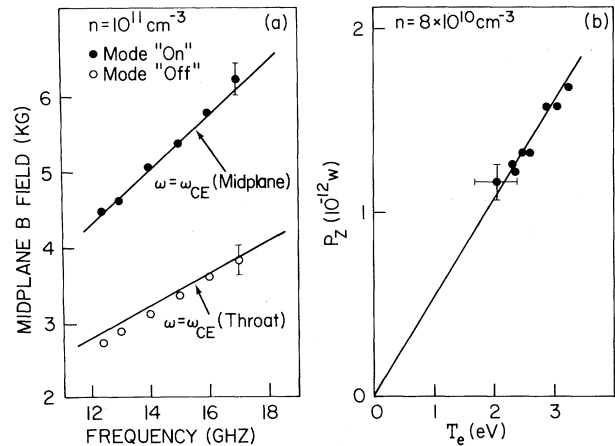


FIG. 3. (a) Magnetic field at midplane vs receiver frequency corresponding to times $t_3$ (solid circles) and $t_4$ (open circles), as indicated in Fig. 2(b). Solid lines are theoretical values for the corresponding cyclotron conditions $\omega = \omega_{ce}$. Discharge voltage 75 V, pressure 0.3 mTorr. (b) Measured mode power $P_z$ vs measured electron temperature, where discharge voltage is varied at a fixed pressure of 0.3 mTorr and fixed density. The error bars are standard deviations for a number of shots. Solid line is fit to data and is extended to $T_e$ = 0 to indicate that it passes through the origin.

shot the receiver frequency is fixed but it can be varied from shot to shot. The mirror region is surrounded by microwave absorber to reduce reflections and this is protected from plasma by a glass tube.

In a mirror field $\omega = \omega_{ce}$ can be satisfied in a number of axial locations depending on the peak value of $\omega_{ce}$. Figure 1 shows the four-zone case $[\omega_{ce}$ (midplane) $< \omega < \omega_{ce}$ (throat)]; one can also have no zones $[\omega_{ce}$ (throat) $< \omega]$ or two zones, both outside the mirror throats $[\omega_{ce}$ (midplane) $> \omega]$. To distinguish between emission from different zones, we use two kinds of "blocks" to isolate zones—a thin mica sheet which terminates the plasma axially, but is transparent to microwaves, and a wire grid transparent to plasma, but opaque to microwaves. Experiments were done with various combinations of block locations and with no blocks.

A typical data shot is shown in Fig. 2 for a case with mica at the mirror throat close to the horn and the grid just on the source side of midplane, isolating zone 3. The time history of the microwave power, $P_z$, is as follows: On the rise of $B$, zone 3 appears at the mirror throat at time $t_1$ and moves toward the midplane, disappearing at time $t_2$; on the fall of $B$, zone 3 reappears at midplane at time $t_3$ and moves to the throat, dis-

appearing at time $t_4$. Any time during the $P_z$ pulse corresponds to emission from a particular axial location between midplane and throat.

We first established that the emission is electron cyclotron radiation, i.e., that it satisfies $\omega = \omega_{ce}$; typical data demonstrating this are shown in Fig. 3(a), where $B$ at midplane corresponding to times $t_3$ and $t_4$ is measured for varying receiver frequency. The solid lines are the $\omega = \omega_{ce}$ conditions and the agreement is excellent. Secondly, we established that received power is proportional to bulk electron temperature. A large variation of $T_e$ is not possible but a factor of the order of 2 can be achieved by varying discharge parameters. In Fig. 3(b) we show measured $P_z$ vs $T_e$, where discharge voltage is varied at constant density; the linear behavior is evident. Similar data obtained by varying neutral pressure yield the same result. Thirdly, we determined that emission is not due to a small population of hot particles by the following measurements: (a) For varying discharge parameters, which change the hot-particle density and energy by more than an order of magnitude, $P_z$ always follows the bulk electron temperature; (b) when the discharge is abruptly terminated during a radiation pulse, hot

particles leave the device in 10 $\mu$s while bulk plasma decays in a time of the order of 100 $\mu$s— the radiation decays on the same time scale as the bulk plasma.

We now turn to the theoretical model. With use of Kirchoff's law, the power received from a radiating slab at temperature $T$ is[1]

$$P = k_B T \Delta f (1 - e^{-\tau}) g, \qquad (1)$$

where $\Delta f$ is the receiver bandwidth, $\tau$ is the optical depth, $k_B$ is Boltzmann's constant, and $g$ is a coupling factor determined by antenna gain, geometry, reflections, waveguide losses, etc. When $\tau \gg 1$, we have $P = k_B T \Delta f g$, and the plasma emits as a black body, so that emission depends only on $T$. The optical depth is related to the imaginary part of the wave vector $k$ using $\tau = \int 2 \mathrm{Im} k \, dl$, where the integral is along a path from a point inside the plasma to the antenna and $\mathrm{Im} k$ is obtained by solving, numerically, the hot-plasma dispersion relation[4,6] for whistler waves for real values of $\omega/\omega_{ce}$. An approximate form for $\tau$ results from noting that at $\omega = \omega_{ce}$ we have

$$k \simeq (\omega/2c)(\sqrt{3} + i)(\sqrt{\pi} \, q/\beta)^{1/3},$$

and that the region of $\omega/\omega_{ce}$, where $\mathrm{Im} k$ is significant, is determined by Doppler broadening and can be approximated by $\Delta \omega/\omega \simeq (\beta c/\omega) \mathrm{Re}(k)$, where

$$\beta = (2k_B T_e/m_e c^2)^{1/2}, \quad q = \omega_p^2/\omega_{ce}^2;$$

the result is valid for $q > \beta$, which encompasses most experiments. Approximating $B$ as $B_0 [1 + (l/L)]$ we obtain

$$\tau \simeq (\sqrt{3} \, \pi^{1/3} \omega/2c) q^{2/3} \beta^{1/3} L,$$

and we see that $\tau$ increases as $n^{2/3} T_e^{1/6}$ so that hotter and denser plasmas are "blacker." The computer code described later uses the numerical solution for $\tau$ rather than this approximate form.

Another method for calculating $\tau$ is based upon noting that an evanescent layer exists between $\omega = \omega_{ce}$ and $\omega = \omega_R$, where $\omega_R$ is the right-hand cutoff defined by $\omega_{ce}/\omega_R = 1 - \omega_p^2/\omega_R^2$. The power absorbed from a wave traversing this layer is computed from the point of view of Budden tunneling[7] and related to $\tau$. The final result is $\tau = \pi(\omega_p^2/\omega)(L/c)$ and this again predicts that denser plasmas are blacker. This result is rigorously valid for a cold plasma and agrees exactly with hot-plasma theory for low densities ($q \ll \beta$).

The calculations of $\tau$ and $g$ have been incorporated, with Eq. (1), into a computer code which predicts the density and temperature dependence

of the power, as well as the detailed shape and magnitude of the $P_z$ pulse. Typical output is shown in Fig. 2(c) along with the experimental data. As can be seen, the agreement is very good with respect to pulse shape. The slight dip in the middle of the pulse is due to the decreasing value of $L$ as the resonant zone moves into the region between the throat and midplane. The slow decrease preceding $t_4$, not described by the code, is probably due to the fact that the resonance zone is approaching the mica block and the density and temperature are falling in this region. The absolute power is in agreement within a factor of 2–3, which represents the difficulty in calculating $g$. Numerous comparisons of this sort have provided good agreement between theory and experiment.

Our most important results are shown in Fig. 4, which shows the variation of received power with plasma density for a wide range of discharge conditions. For each set of conditions $P_z$ has been normalized to the saturated value at high densities to account for small changes in $T_e$. Also shown are the theoretical models, where $\tau$ is calculated using hot-plasma theory and Budden tunneling. Note the approach to blackness as the density is increased and the subsequent saturation at higher densities, features which both theories agree upon. The only difference is related to the approach to black-body levels and considering the scatter in the data, both models are in good agreement with the experiment, but the hot-plasma result appears to be in slightly better agreement. The measured radial variation of density has been included by integrating Eq. (1) over radius to give $P_z = \int P(r) 2\pi r \, dr$; to a good approximation, our experimental radial density pro-
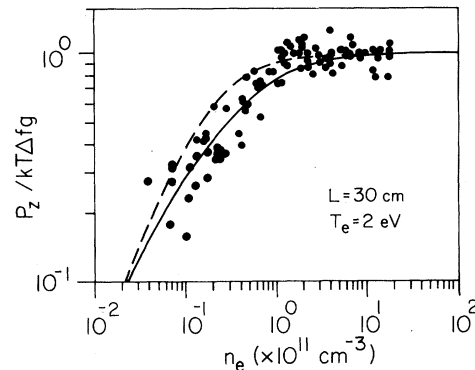


FIG. 4. Measured mode power, normalized to $kT\Delta fg$, vs plasma density (dots). Solid line is prediction of hot-plasma theory, dashed line is prediction of Budden tunneling theory.

file can be represented by a parabola. Our calculation does not treat radial refraction. The use of a high-gain antenna and the flatness of the absorption coefficient for small angles around the direction of the magnetic field justifies the one-dimensional calculation. Corrections due to refraction are under investigation.

Another important issue is that of propagation and accessibility. At modest-to-high plasma densities the whistler mode can propagate to the horn only if $\omega < \omega_{ce}$ along the entire path because of the evanescent region for $\omega_{ce} < \omega < \omega_R$. For example, referring to Fig. 1, radiation from resonance zone 2 and the portion of zone 1 for which $\omega > \omega_{ce}$ (midplane) cannot reach the antenna. At very low densities, tunneling through the cutoff layer becomes possible. These points have been confirmed in detail by manipulating the positions of the blocks described earlier.

Finally, when our model is applied to the plasma expected on TMX Upgrade[3] we find that the radiation achieves black-body levels for all projected conditions in both the end cells and the center cell, thus confirming the utility of this mode as a temperature diagnostic. Of course, the propagation and accessibility constraints imply that only those regions of the device for which $\omega < \omega_{ce}$ along the entire path to the antenna are visible. This still allows a considerable portion of the device to be viewed, and reduces the problem of emission from different resonant zones. We note that on large mirror devices the antenna will be located in a weak-field region some distance from the mirror throat, in a manner identical to that of our experiment. On such devices the plasma density outside the mirror will be quite low and absorption and emission in this region should not be a problem. Detailed results applying to TMX Upgrade will be published at a later date.

In conclusion, we have made the first measurements of electron cyclotron emission along the magnetic field lines in the whistler mode and compared these results with the relevant theoretical models. The results are in good agreement with the predictions of hot-plasma theory and the applications of this mode to the problem of axial temperature measurements on large mirror machines appear extremely promising.

[1]G. Bekefi, *Radiation Processes in Plasma* (Wiley, New York, 1966).

[2]A. E. Costley, R. J. Hastie, J. W. M. Paul, and J. Chamberlain, Phys. Rev. Lett. **33**, 758 (1974); D. A. Boyd, F. J. Stauffer, and A. W. Trivelpiece, Phys. Rev. Lett. **37**, 98 (1976); C. M. Celata and D. A. Boyd, Nucl. Fusion **17**, 735 (1977).

[3]D. E. Baldwin and B. G. Logan, Phys. Rev. Lett. **43**, 1318 (1979); F. G. Coensgen, T. C. Simonen, A. K. Chargin, and B. G. Logan, Lawrence Livermore Laboratory Report No. LLL-PROP-172, 1980 (unpublished).

[4]T. H. Stix, *The Theory of Plasma Waves* (McGraw-Hill, New York, 1962), pp. 38–40, 193–196.

[5]G. D. Tsakiris, D. A. Boyd, D. A. Hammer, A. W. Trivelpiece, and R. C. Davidson, Phys. Fluids **21**, 2050 (1978).

[6]V. L. Ginzburg, *The Propagation of Electromagnetic Waves in Plasmas* (Pergamon, Oxford, 1970), pp. 166–171; C. L. Olson, Phys. Fluids **15**, 160 (1972).

[7]K. G. Budden, *Radio Waves in the Ionosphere* (Cambridge Univ. Press, Cambridge, 1961), p. 476; D. B. Batchelor, Plasma Phys. **22**, 41 (1980).